Electron paramagnetic resonance of phosphate-derived radicals in KCl



1992 J. Phys.: Condens. Matter 4 6593

(http://iopscience.iop.org/0953-8984/4/31/011)

J. Phys.: Condens. Matter 4 (1992) 6593–6602. Printed in the UK

# Electron paramagnetic resonance of phosphate-derived radicals in KCl

F Callens, F Maes, P Moens, P Matthys and E Boesman

Laboratorium voor Kristallografie en Studie van de Vaste Stof, Krijgslaan 281, S1, B-9000 Gent, Belgium

Received 12 March 1992, in final form 7 May 1992

**Abstract.** We examined the EPR spectrum of KCl single crystals doped with either $K_3PO_4$ or $P_2O_5$ after x-ray or neutron irradiation. Two new related $O^-$ defects and two phosphorus-containing radicals were detected. One of the latter is identified as a $PO_2^{2-}$ radical in an anion vacancy.

## 1. Introduction

During our investigations of isoelectronic paramagnetic oxides and oxyions of the non-metals (e.g. NO; $CO_2^-$, $NO_2$; $CO_3^-$, $NO_3$; etc) in alkali halides we found it striking that very little is known about phosphate-derived radicals (PO, $PO_2$, $PO_3$, $PO^{2-}$, etc). Indeed $^{31}P$ (nuclear spin $I = \frac{1}{2}$) has a natural abundance of 100% which allows rather easy identification and inexpensive possibilities for studying the $^{31}P$ hyperfine interactions. On the other hand a nearly overwhelming number of nitrate- and nitrite-derived paramagnetic defects were reported in alkali halides [1–4].

Our interest in the phosphorus-centred radicals originates also from our studies of biological and synthetic carbonate-containing hydroxyapatites $Ca_{10}(OH)_2(PO_4)_6$. Even in these lattices, very few phosphate-derived paramagnetic defects contribute to the EPR spectra except for $PO_4^{2-}$ after irradiation at low temperatures (e.g. 77 K). A general literature search, however, yields EPR data concerning $PO_4^{2-}$, $PO_3^{2-}$, $PO_2^{2-}$, $PO_3$ and $HPO_2^-$ [5–10].

In this paper we discuss our results on both Kyropoulos- and Bridgman-grown KCl crystals doped with either $K_3PO_4$ or $P_2O_5$. A comparison with other isoelectronic defects is made.

## 2. Experimental details

On the one hand, KCl crystals were grown using the Kyropoulos method. 1.6 wt% $K_3PO_4.3H_2O$ (Merck) was dried at 200 °C and added to the alkali halide powder. On the other hand, KCl single crystals were prepared by the Bridgman method. Doping with either 0.1 wt% $K_3PO_4.3H_2O$ or $P_2O_5$ was carried out after drying the starting materials at 250 °C.

The x-irradiations were performed with a Philips tungsten anticathode x-ray tube, operated at 60 kV and 40 mA. Typical irradiation doses are 10–50 kGy. Neutron

0953-8984/92/316593+10$04.50  

irradiations were carried out at room temperature at a mean energy of 0.025 eV for about 1 h in a flux of $1.6 \times 10^{12}$ cm$^{-2}$ s$^{-1}$.

The EPR spectra were recorded using a Bruker ESP300 X-band spectrometer with 200 mW maximum power available. The magnetic field was modulated at 100 kHz with a peak-to-peak amplitude of 0.1 mT. All spectra were normalized to the same frequency, namely 9.47 GHz. Temperatures down to approximately 2 K could be realized by means of an Oxford Instruments ESR10 flow cryostat.

## 3. EPR results

### *3.1. Kyropoulos crystal KCl:$K_3PO_4.3H_2O$ (1.6 wt%)*

In spite of intensive searching, no EPR spectra due to phosphorus-centred radicals could be detected after x-irradiation. The latter was performed at room and at liquid-nitrogen temperature. Since, for example in $CaCO_3$ [5], $PO_3^{2-}$ was produced after neutron irradiation, we tried such a treatment also. Again no phosphate-derived radicals were found. Nevertheless a spectrum (labelled S1) exhibiting no hyperfine structure could be studied at about 2 K and 0.01 mW microwave power. In figure 1 the angular dependence of the S1 resonances is presented with $\boldsymbol{B}$ in a $\{100\}$ plane, showing monoclinic **g**-tensor symmetry; one **g** tensor axis ($y$ axis) is along $\langle 001 \rangle$ while the $x$ and $z$ axes are tilted 5° away from $\langle 110 \rangle$ and $\langle 1\bar{1}0 \rangle$, respectively (table 1).

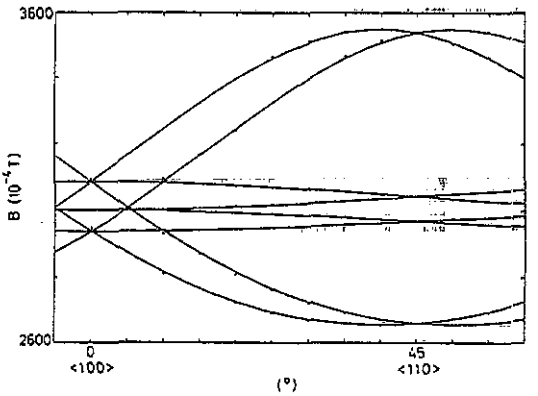


**Figure 1.** Angular variation in the S1 EPR resonance positions in a $\{100\}$ plane. The full curves are calculated with the **g**-tensor in table 1.

**Table 1.** **g**-tensor of defect S1. The direction cosines $L$, $M$ and $N$ are referred to the crystal axes.

| | $g$ | $L$ | $M$ | $N$ |
|---|---|---|---|---|
| $x$ | 2.5470 | 0.642 788 | 0.766 045 | 0 |
| $y$ | 2.2539 | 0 | 0 | 1 |
| $z$ | 1.9056 | 0.766 045 | −0.642 788 | 0 |

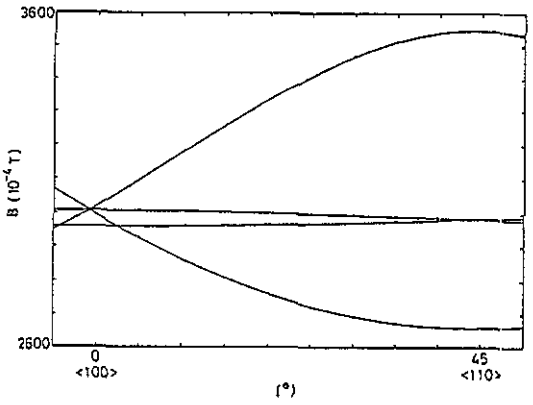


**Figure 2.** Angular variation in the S2 spectrum in a {100} plane. The full curves are calculated with the **g**-tensor in table 2.

### *3.2. Bridgman crystal KCl:$K_3PO_4.3H_2O$ (0.3 wt%)*

In these crystals, several spectra could be observed after x-irradiation at room temperature (XRT). One spectrum (labelled S2) is best detectable at 5 K and 1 mW microwave power and exhibits orthorhombic **g**-tensor symmetry. The **g**-tensor principal axes are oriented along $\langle 110\rangle$, $\langle 1\bar{1}0\rangle$ and $\langle 001\rangle$ (table 2 and figure 2).

**Table 2.** **g**-tensor of defect S2.

| $g_x\langle 110\rangle$ | $g_y\langle 001\rangle$ | $g_z\langle 1\bar{1}0\rangle$ |
|---|---|---|
| 2.5453 | 2.2855 | 1.9071 |

The close resemblance between the **g**-tensor principal values of S1 and S2 is striking. Only the orientations of the $g_x$ and $g_z$ axes are slightly different for both centres.

In the same crystal, two other spectra are characterized by a hyperfine splitting with $I = \frac{1}{2}$, probably originating from phosphorus-centred radicals with one $^{31}P$ nucleus. One of these spectra (P1) is weakly visible at room temperature but the variation in the line positions is small compared with the linewidth so that the spin-Hamiltonian parameters could only be roughly estimated:

$$g_\perp = 2.003 \pm 0.001 \qquad A_\perp = 170 \pm 30\,\mathrm{MHz}$$
$$g_\parallel = 2.002 \pm 0.001 \qquad A_\parallel = 112 \pm 30\,\mathrm{MHz}.$$

The P1 spectrum depends in a very peculiar way on the irradiation time. It is not visible without XRT but after irradiations longer than about 2 min (approximate dose, 2 kGy) the intensity of the spectrum decreases again.

The second spectrum with hyperfine structure (P2) was best detectable near 20 K and 0.01 mW. We averaged the EPR signals five times to increase the signal-to-noise ratio. In figures 3(*a*) and 3(*b*) the spectra are presented for $B\|\langle 100\rangle$ and $B\|\langle 110\rangle$, respectively. In figure 4 the experimental angular variation is fitted with the spin-Hamiltonian parameters of table 3.

The choice of the signs for the hyperfine (HF) parameters will be discussed below. The same P2 spectrum was found in Bridgman crystals doped with $P_2O_5$.

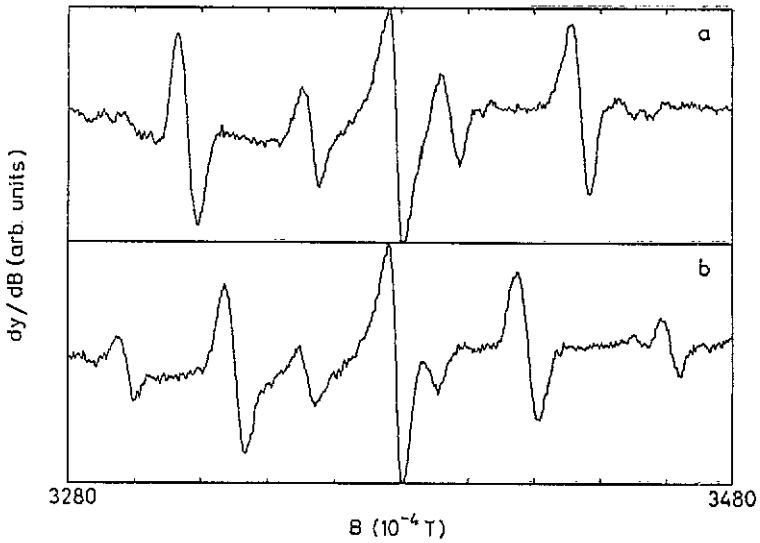


**Figure 3.** (*a*) EPR spectrum of defect P2 with $B\|\langle 100\rangle$. (*b*) EPR spectrum of defect P2 with $B\|\langle 110\rangle$. The central line around $g = 2.0023$ does not belong to the P2 spectrum.

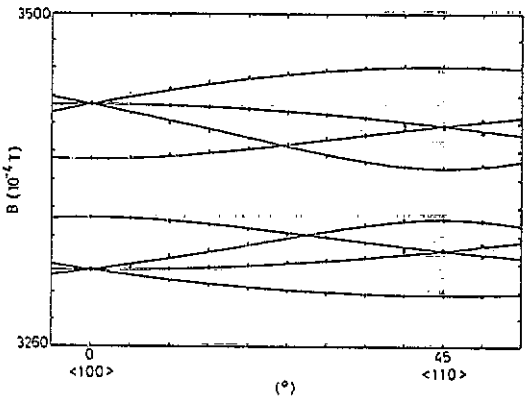


**Figure 4.** Angular variation in the P2 spectrum in a {001} plane. The full curves are calculated with the spin Hamiltonian in table 3.

**Table 3.** Spin-Hamiltonian parameters of defect P2.

| | $g$ | $A$ (MHz) |
|---|---|---|
| $x\langle 110\rangle$ | 2.0021 | 458.8 |
| $y\langle 110\rangle$ | 2.0071 | 98.3 |
| $z\langle 001\rangle$ | 2.0050 | 117.9 |
| Average | 2.0047 | 225.0 |

## 4. Discussion

Although both crystal growth methods are rather different (air contact for Kyropoulos, and vacuum for Bridgman), it remains unclear why the S1 spectrum occurs only in

Kyropoulos-grown crystals while the opposite is true for the S2, P1 and P2 defects. As the P1 and P2 spectra are weak, it might be only a matter of concentration in this case. As will become clear, S1 and S2 are in fact the same defect although we do not understand the reason for the slightly different **g**-tensor axes. The above certainly illustrates the fact that the production of paramagnetic phosphate centres in alkali halides is in general poorly understood.

### *4.1. S1 and S2 centres*

As the spectra of these two centres show no doublet splitting due to the $^{31}P$ ($I = \frac{1}{2}$) nucleus, oxygen centres are most probable in view of the doping with $K_3PO_4$. In addition we suspect that the same defect accounts for both the S1 and the S2 spectra because of their very similar **g**-tensors. A glance at the literature reveals that $O_2^-$ and $O_3^-$ ions whose **g**-tensors have also $D_{2h}$ symmetry can be ruled out; the **g**-tensor of $O_2^-$ is nearly axial with two principal $g$-values smaller than $g_e = 2.0023$ [11], while the **g**-tensor of $O_3^-$ is characterized by a small anisotropy and three principal values larger than $g_e$ [12, 13]. On the other hand the **g**-tensor values of S1 and S2 correspond very well qualitatively and even quantitatively to those of some $O^-$ centres in alkali halides [14, 15].

The theory for a $p^5$ ($^2P$) configuration was well established by Vannotti and Morton [16] and yields the following principal **g**-tensor values:

$$g_x = g_e(-A^2 + B^2 + C^2) + 4lBC$$

$$g_y = g_e(A^2 - B^2 + C^2) + 4lAC$$

$$g_z = g_e(-A^2 - B^2 + C^2) + 4AB$$

where $A$, $B$, $C$ and $l$ are adjustable parameters (for more details see [16]).

As could be expected, both **g**-tensors can be perfectly interpreted in terms of the above equations. Hence we suggest that both S1 and S2 centres are essentially $O^-$ ions in slightly different surroundings. Since the **g**-tensor principal axes of the S2 centre are simple crystallographic orientations, we propose a substitutional site for this defect, in agreement with the KCl:$S^-\langle 110\rangle$ model of Vannotti and Morton [16]. In fact it is baffling to see that the **g**-tensors of the latter $S^-\langle 110\rangle$ centre and of the S2 model are nearly identical. By doping with sulphur enriched with $^{33}S$ ($I = \frac{3}{2}$) the identification of the Vannotti–Morton $S^-\langle 110\rangle$ model was firmly established. Ascribing S2 to some sulphur centre due to accidential contamination is nevertheless highly improbable because the S2 lines are very strong and no trace of optical $S^-$ bands were found. Furthermore a comparable coincidence between the KCl:$O_2^-$ [11] and KCl:$S_2^-$ **g**-tensor values and **g**-tensor axes was already mentioned in [17]. In that case, however, both $^{17}O$ [11] and $^{33}S$ enrichment [17] could exclude any misidentification.

As far as the S1 resonances are concerned, we think that they arise from a substitutional $O^-$ in perturbed surroundings, caused by radiation damage following neutron irradiation. More detailed models seem too speculative in view of the lack of experimental information such as ENDOR data.

### *4.2. Introductory remarks concerning the P1 and P2 centres*

Both the P1 and the P2 EPR spectra can be interpreted in terms of radicals containing only one $^{31}P$ nucleus (natural abundance, 100%). *A priori* eight reasonable possibilities can be considered: PO, $PO_2$, $PO_3$, $PO_4$ and $PO^{2-}$, $PO_2^{2-}$, $PO_3^{2-}$, $PO_4^{2-}$. Cations

are improbable in view of the doping procedure and in view of the EPR results on related molecules and molecular ions.

The $PO_3^{2-}$ and $PO_2$ possibilities can be safely eliminated because of their large hyperfine splittings. This can be simply explained as for both radicals the unpaired electron occupies a molecular orbital with $A_1$ symmetry, yielding large $^{31}P$ HF values due to the contribution of the $3s_p$ atomic orbital. Experimentally one finds for example $CaCO_3$:$PO_3^{2-}$ splittings exceeding 1700 MHz [5]. The $PO_2$ molecule is isoelectronic with for example $NO_2$ and $CO_2^-$ which have already been studied in alkali halides and particularly in KCl [4, 18]. Considering table 4, we expect the HF splittings of phosphorus-containing radicals to be roughly six and three times larger than the corresponding nitrogen- and carbon-containing radicals, respectively. As the splittings of $^{13}CO_2^-$ already exceed 300 MHz, a $PO_2$ model for either P1 or P2 is very improbable too.

Next to the pair $PO_2$–$PO_3^{2-}$ we shall consider the $PO_3$–$PO_4^{2-}$ and PO–$PO_2^{2-}$ pairs. These pairs differ only in an $O^{2-}$ ion with a noble gas configuration and are often mixed up because they are nearly indistinguishable on the basis of simple theoretical arguments (see later and [19, 21–24]).

**Table 4.** Calculated hyperfine couplings and spin–orbit coupling constants for a few nuclei with $I \neq 0$ [19, 20], where $A_0 = (\mu_0/4\pi)(8\pi/3)(g_N\beta_N g_e\beta/h)|\Psi_s(0)|^2$ and $B_0 = (\mu_0/4\pi)\frac{2}{5}(g_N\beta_N g_e\beta/h)\langle r^{-3}\rangle_p$.

| | $A_0$ (MHz) | $B_0$ (MHz) | $\lambda$ ($cm^{-1}$) |
|---|---|---|---|
| $^{13}C$ | 3108.66 | 90.56 | 29 |
| $^{14}N$ | 1538.22 | 47.73 | 76 |
| $^{17}O$ | −4626.26 | −143.69 | 151 |
| $^{31}P$ | 10 188.28 | 286.00 | 299 |
| $^{33}S$ | 2728.01 | 78.97 | 382 |
| $^{75}As$ | 9531.32 | 254.45 | 1550 |
| $^{77}Se$ | 13 419.78 | 377.85 | 1688 |

$PO^{2-}$ is isoelectronic with $O_2^-$, $S_2^-$, $Se_2^-$ and $SSe^-$ with a **g**-tensor behaviour clearly different from those found for P1 and P2; these four ions have two $g$-values smaller than $g_e$ in alkali halides [11, 25, 26]. In the literature, nothing is known about $PO_4$ so that we shall confine ourselves to the discussion of the $PO_3$–$PO_4^{2-}$ and PO–$PO_2^{2-}$ pairs. As will be argued below, the P1 spectrum probably belongs to the former, and the P2 spectrum to the latter pair. Figure 5 is very illustrative in this respect and will be further explained in the section concerning the P2 centre.

### *4.3. P1 centre*

From the literature it is known that the $PO_3$ and $PO_4^{2-}$ radicals have smaller HF values than the PO–$PO_2^{2-}$ pair to be discussed in the next section. $PO_3$ is isoelectronic with $CO_3^-$ and $NO_3$ which we know from the literature and our own experience in alkali halide single crystals. The P1, $CO_3^-$ and $NO_3$ defects are all formed after XRT, are visible at RT and decay rather quickly. The latter two radicals which have 23 valence electrons are also both characterized by small HF splittings and anisotropy ($\langle A\rangle \simeq 30$ MHz and 10 MHz for $CO_3^-$ and $NO_3$, respectively) which can be adequately explained by their $^2A_2'$ ground state. The non-zero isotropic HF splitting arises

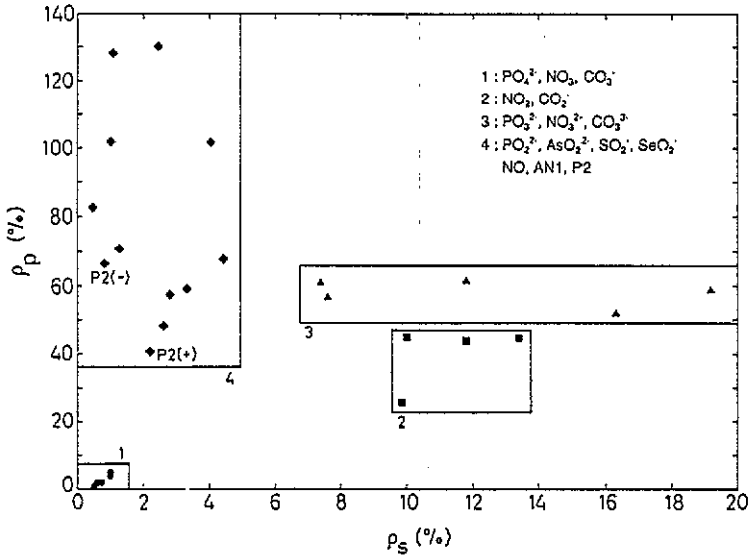


**Figure 5.** s and p fractions of the unpaired spin density for molecules and molecular ions isoelectronic with $PO_3$, $PO_4^{2-}$ (block 1), $PO_2$ (block 2), $PO_3^{2-}$ (block 3) and PO, $PO_2^{2-}$ (block 4). In block 4 the P2 values are indicated for the + and − choice of HF constants.

completely from spin polarization effects. As discussed by Atkins and Symons [19], the same is true for $AB_4$ species with 31 valence electrons such as $PO_4^{2-}$. Isotropic HF splittings ranging from 55 to 140 MHz were reported [5, 10], in agreement with the P1 HF tensor. As our experimental results are only partial we shall not speculate about either a $PO_3$ or a $PO_4^{2-}$ model. Nevertheless we believe that the considerations about $PO_3$ and $PO_4^{2-}$ are also useful to exclude them as possibilities for the P2 centre with a definitely larger isotropic HF splitting of about 225 MHz and especially a strong anisotropy of the hyperfine tensor.

### *4.4. P2 centre*

By excluding the other possibilities we are left with PO and $PO_2^{2-}$ as possible candidates for the P2 centre. However, we shall corroborate this assignment by a positive argument also.

The spin Hamiltonian of the P2 radical (table 3) is very similar to that of a nitrogen-containing radical that was found in KCl (and KBr) by several workers [1–3]. The spin Hamiltonian of this AN1 centre (assigned to an interstitial NO molecule) is included in table 5.

Considering table 4 it is found that the **A**-tensor of the P2 centre is to a very good approximation the same as for AN1, taking into account the proportionality factor between the $A_0$- and $B_0$-values for $^{31}P$ and $^{14}N$. Also the **g**-tensor principal values are in qualitative agreement. Only the orientation of minimum $g$ and maximum $A$ corresponds to ⟨110⟩ for our P2 defect at variance with the AN1 defect. Provided that this model for AN1 [1–3] is correct, one is tempted to identify the P2 centre as a PO molecule oriented along ⟨110⟩ in a positive or negative vacancy. Without going into details we mention, however, that the assignment of several spectra to NO (including AN1) has been strongly criticized. Many workers agree that an $NO_2^{2-}$

**Table 5.** Comparison of isoelectronic defects ($\langle A \rangle$ is the isotropic part of the HF tensor [1, 7, 13, 28–30]. The $\langle 110 \rangle$, $\langle 1\bar{1}0 \rangle$ and $\langle 001 \rangle$ axes apply only to the centres in alkali halides.

| | $g\langle 110 \rangle$ | $g\langle 1\bar{1}0 \rangle$ | $g\langle 001 \rangle$ | $A\langle 110 \rangle$ (MHz) | $A\langle 1\bar{1}0 \rangle$ (MHz) | $A\langle 001 \rangle$ (MHz) | $\langle A \rangle$ (MHz) |
|---|---|---|---|---|---|---|---|
| AN1 (KCl) | 2.0070 | 2.0099 | 2.0038 | 19.7 | 14.1 | 86.6 | 40.0 |
| $O_3^-$ (KBr) | 2.0027 | 2.0180 | 2.0113 | — | — | — | — |
| $SO_2^-$ (KCl) | 2.0025 | 2.0110 | 2.0071 | 147 | −20 | −24 | 35 |
| $SO_2^-$ ($BaSO_4$) | 2.0032 | 2.0128 | 2.0104 | 151 | −20 | −23 | 36 |
| $SeO_2^-$ (KCl) | 1.9989 | 2.0367 | 2.0165 | 688 | −237 | −254 | 65 |
| $SeO_2^-$ [29] | | | | 670 | −240 | −269 | 54 |
| P2 (KCl) | 2.0021 | 2.0071 | 2.0050 | 458 | ±98 | ±118 | 225 |
| $AsO_2^{2-}$ ($CaCO_3$) | 1.9991 | 2.0150 | 1.9910 | 614 | ±152 | ±173 | 313 |
| $PO_2^{2-}$ ($BaSO_4$) | 1.9992 | 2.0037 | 1.9992 | 840 | ±258 | ±255 | 451 |
| $PO_2^{2-}$ ($P_2O_5$) | 2.0014 | 1.9989 | 1.9989 | 994 | ±122 | ±122 | 413 |

model is preferable (see, e.g., [1–3, 10, 19, 22, 27]).

The $NO_2^{2-}$ ion with 19 valence electrons is isoelectronic with for example $PO_2^{2-}$, $SO_2^-$ and $O_3^-$ and the unpaired electron is expected to reside in a $b_1$ ($\pi^*$) molecular orbital:

$$|b_1\rangle = -c_1 p_{x\mathrm{N}} + c_2(p_{x1} + p_{x2})/\sqrt{2}$$

$p_{x\mathrm{N}}$, $p_{xi}$ ($i = 1, 2$) are nitrogen and oxygen atomic $p_x$ orbitals, respectively. The $x$ direction is as usually chosen perpendicular to the molecular plane; the $y$ direction is along the O–O axis.

It immediately follows that $g_x$ approximates very closely to $g_e$, in fair agreement with the $g\langle 100 \rangle$-value of AN1 (table 5). It can be shown that $g_y$ (O–O direction) and $g_z$ are both larger than $g_e$, also in agreement with table 5. The isotropic HF splitting should be small and due to polarization phenomena. The HF tensor should exhibit considerable anisotropy with the largest splitting along the $x$ direction. As a result we can state that indeed the AN1 spectrum can be explained by an $NO_2^{2-}$ model.

The spin Hamiltonian of P2 is thus also in excellent qualitative agreement with a $PO_2^{2-}$ model, in view of the already mentioned similarity between the AN1 and P2 spin Hamiltonians. In table 5 we compare the spin-Hamiltonian data of several molecular ions isoelectronic with $PO_2^{2-}$. It is found that the **g**-tensor of P2 fits in very well. For the HF data we are faced with several possibilities for the signs of the $A$-values. The only signs that were determined with certainty are those for $SO_2^-$ and $SeO_2^-$ in KCl, and the AN1 spectrum as the corresponding isotropic spectra could be observed at higher temperatures [1–3, 28]. For the other ions we included two reasonable choices of the signs (all $A$-values positive or the two smallest $A$-values negative). For $SeO_2^-$ we changed the sign choices mentioned in [29], yielding close agreement with the well established values for KCl:$SeO_2^-$. In the original paper, two $A$-values were taken as negative for $AsO_2^{2-}$ [30] while for $PO_2^{2-}$ [7, 10] both choices occur. Using the $A_0$- and $B_0$-values in table 4, we calculated the s and p contributions ($\rho_s$ and $\rho_p$) to the unpaired spin density for the ions in table 5. These values were plotted in figure 5 in a $\rho_p, \rho_s$ diagram together with a fairly representative set of experimental data for the distinct types of molecule and molecular ion that reasonably can be considered for P2 [1–10, 19, 23, 24, 28–30]. It follows that in

spite of the large spread in $\rho_p$-values the group of defects isoelectronic with $PO_2^{2-}$ or PO are well separated from $PO_4^{2-}$, $PO_3$, $PO_3^{2-}$ and $PO_2$ (solely on the base of the **A**-tensor). Taking also into account the **g**-tensor considerations about NO and $NO_2^{2-}$ made above and in the literature [19, 22, 27] we believe that the P2 spectrum can be best explained in terms of a $PO_2^{2-}$ model.

In the alkali halides the $O_3^-$, $SO_2^-$ and $SeO_2^-$ ions are located in an anion vacancy site. As the non-paramagnetic $PO_2^-$ ion was already identified in unirradiated KCl [29] with an orientation in the lattice that corresponds perfectly to the **g**-tensor axes for the P2 defect, the identification as $PO_2^{2-}$ is even corroborated. The latter paramagnetic defect can be formed by simply trapping an electron during the x-irradiation.

## 5. Conclusion

Irradiation of phosphate-doped KCl single crystals yields two related $O^-$ centres at anion sites. We have insufficient experimental data to decide between a $PO_3$ or $PO_4^{2-}$ model for a phosphorus-containing radical that is weakly detectable at RT. The second phosphorus-containing and the most interesting defect is probably a $PO_2^{2-}$ radical in an anion vacancy, in agreement with the models established earlier for the isoelectronic $O_3^-$, $SO_2^-$ and $SeO_2^-$ ions in alkali halides. A PO model is considered to be less probable and we agree with several workers that earlier spectra assigned to KCl:NO and KBr:NO can be more adequately interpreted in terms of an $NO_2^{2-}$ model. In any case the hyperfine tensors of the paramagnetic defects isoelectronic with PO or $PO_2^{2-}$ are rather sensitive to the host lattice.

## Acknowledgments

The authors wish to thank Professor Dams and Dr Piens (INW) for the neutron irradiation of some of our samples. This work is part of a project sponsored by the Executieve van de Vlaamse Gemeenschap, Departement Onderwijs, which is gratefully acknowledged. F Callens is a Research Associate of the NFSR (Belgium).

## References

[1] Jaccard C 1961 *Phys. Rev.* **124** 60–6
[2] Schoemaker D and Boesman E 1963 *Phys. Status Solidi* **3** 1695–703
[3] Schoemaker D 1962 *PhD Thesis* RUG, Gent
[4] Brailsford J R and Morton J R 1968 *J. Magn. Reson.* **1** 575–83
[5] Serway R A and Marshall S A 1966 *J. Chem. Phys.* **45** 4098–104
[6] Horsfield A, Morton J R and Whiffen D H 1961 *Mol. Phys.* **4** 475–80
[7] Ryabov I D, Bershov L V and Ganeev I G 1989 *Phys. Chem. Min.* **16** 374–7
[8] Hanna M W and Altman L J 1962 *J. Chem. Phys.* **36** 1788–92
[9] Morton J R 1962 *Mol. Phys.* **5** 217–23
[10] *Landolt–Börnstein New Series* 1987 Zahlenwerte und Funktionen aus Naturwissenschaften und Technik, Group II, Atom- und Molekularphysik vol 17a (Berlin: Springer) pp 87, 89
[11] Zeller H R and Känzig W 1967 *Helv. Phys. Acta* **40** 845–72
[12] Callens F, Matthys P and Boesman E 1988 *J. Phys. C: Solid State Phys.* **21** 3159–64
[13] Maes F, Callens F, Matthys P and Boesman E 1989 *Phys. Status Solidi* b **155** K55–7
[14] Sander W 1962 *Z. Phys.* **169** 353–63
[15] Brailsford J R and Morton J R 1969 *J. Chem. Phys.* **51** 4794–8

[16] Vannotti L E and Morton J R 1968 *Phys. Rev.* **174** 448–53
[17] Callens F, Maes F, Matthys P and Boesman E 1989 *J. Phys.: Condens. Matter* **1** 6921–8
[18] Callens F, Matthys P and Boesman E 1989 *J. Phys. Chem. Solid.* **50** 377–81
[19] Atkins P W and Symons M C R 1967 *The Structure of Inorganic Radicals* (Amsterdam: Elsevier) pp 148–50
[20] Koh A K and Miller D J 1985 *At. Data Nucl. Data Tables* **33** 235–53
[21] Owens F J 1971 *Chem. Phys. Lett.* **12** 92–4
[22] Fuller A M and Tarr C E 1972 *J. Chem. Phys.* **56** 438–40
[23] Callens F J, Verbeeck R M H, Naessens D E, Matthys P F A and Boesman E R 1989 *Calc. Tissue Int.* **44** 114–24
[24] Callens F J, Verbeeck R M H, Naessens D E, Matthys P F A and Boesman E R 1991 *Calc. Tissue Int.* **48** 249–59
[25] Maes F, Matthys P, Callens F, Moens P and Boesman E 1992 *J. Phys.: Condens. Matter* **4** 249–56
[26] Vannotti L E and Morton J R 1967 *Phys. Lett.* **24** A 520–1
[27] Symons M C R 1962 *Adv. Chem. Ser.* **36** 7–8
[28] Schneider J, Dischler B and Räuber A 1966 *Phys. Status Solidi* **13** 141–57
[29] Hunter S J, Hipps K W and Francis A H 1979 *Chem. Phys.* **40** 367–75
[30] Marshall S A and Serway R A 1969 *J. Chem. Phys.* **50** 435–9